

Supplement of

Subglacial lake activity beneath the ablation zone of the Greenland Ice Sheet

Yubin Fan et al.

Correspondence to: Chang-Qing Ke (kecq@nju.edu.cn)

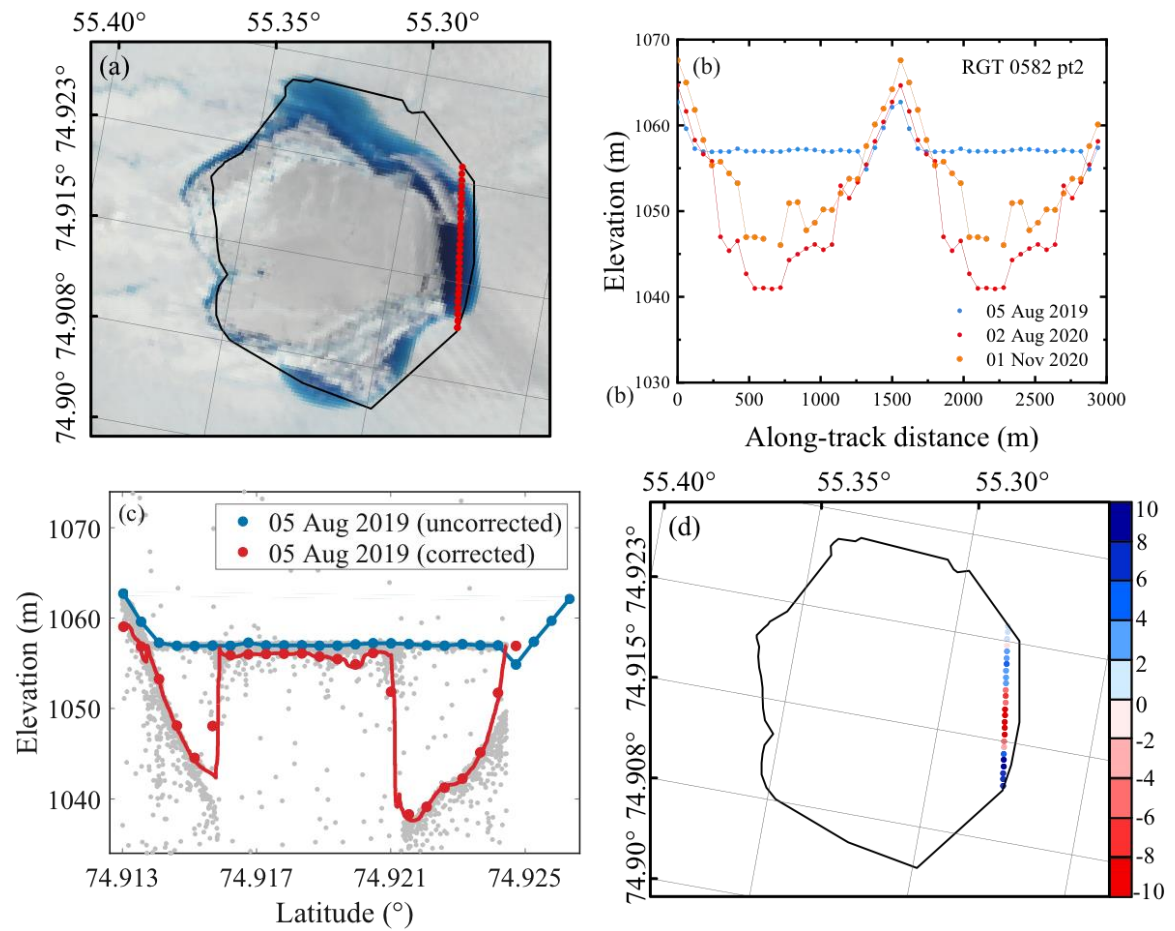


Figure S1. An example of ice-surface height correction based on ICESat-2 ATL03 data. (a) ICESat-2 ATL 11 track overlaid on a Landsat-8 image acquired on 08 August 2019, showing a supraglacial lake. (b) Elevation anomaly profile across the subglacial lake along the ICESat-2 track, removing the cycle acquired on 02 February 2020 since it has a flat spot and cannot be corrected. (c) Original ICESat-2 ATL03 photon data collected over the lake on 08 August 2019. The top and bottom of the double reflection correspond to the lake surface and bottom, and the flat spot in the middle of the red line reflects the ice surface. The corrected elevation of ATL11 data is shown in red. (d) indicate the elevation-change rate over the track after the correction.

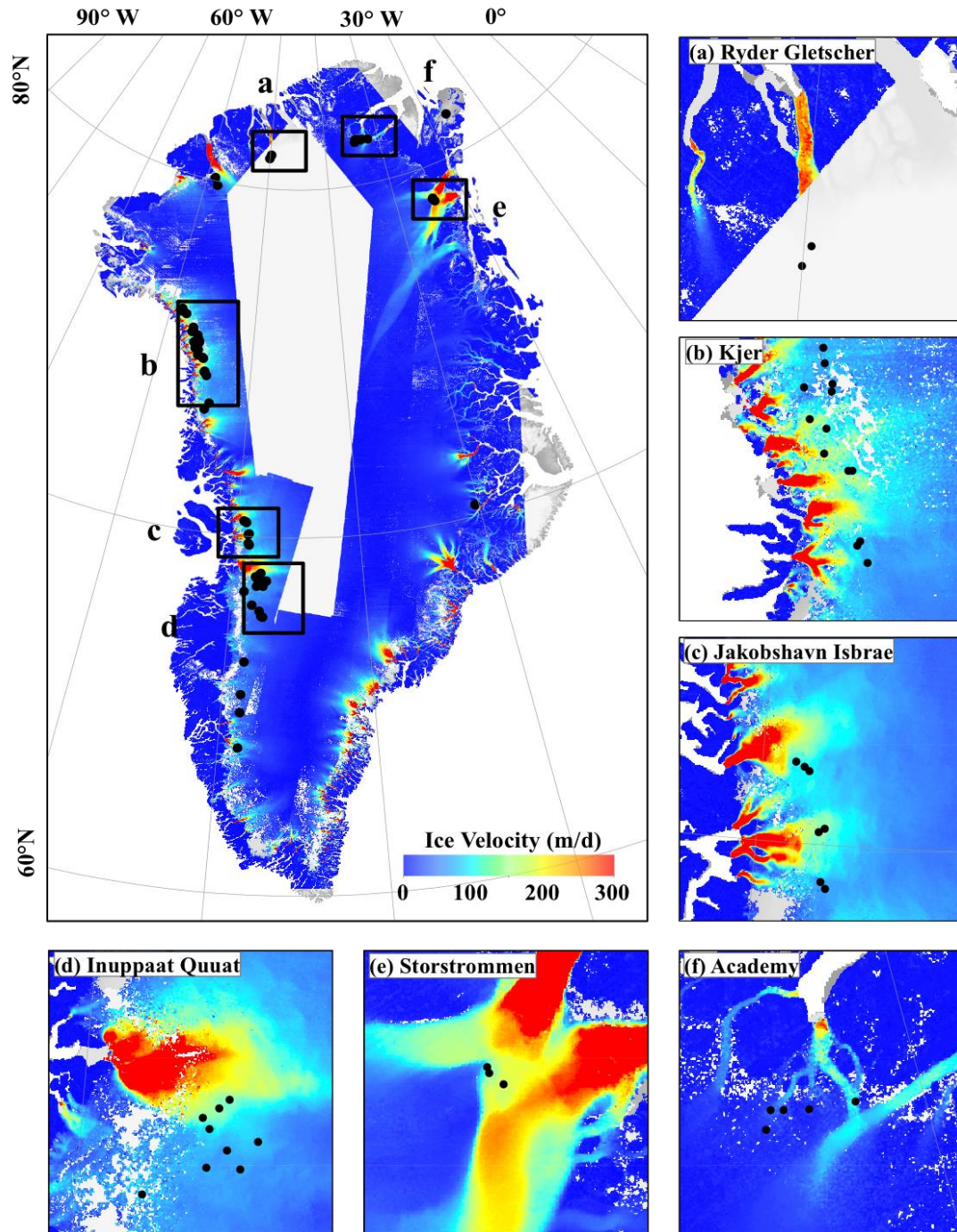


Figure S2. Examples of the spatial distribution of subglacial lakes across selected regions of the Greenland Ice Sheet. (a) Ryder Gletscher, (b) Kjer, (c) Jakobshavn Isbrae, (d) Inuppaat Quuat, (e) Storstrommen and (f) Academy. Background shows a Sentinel-1-derived ice velocity from 10 August 2020 to 03 September 2020 (Solgaard et al., 2021).

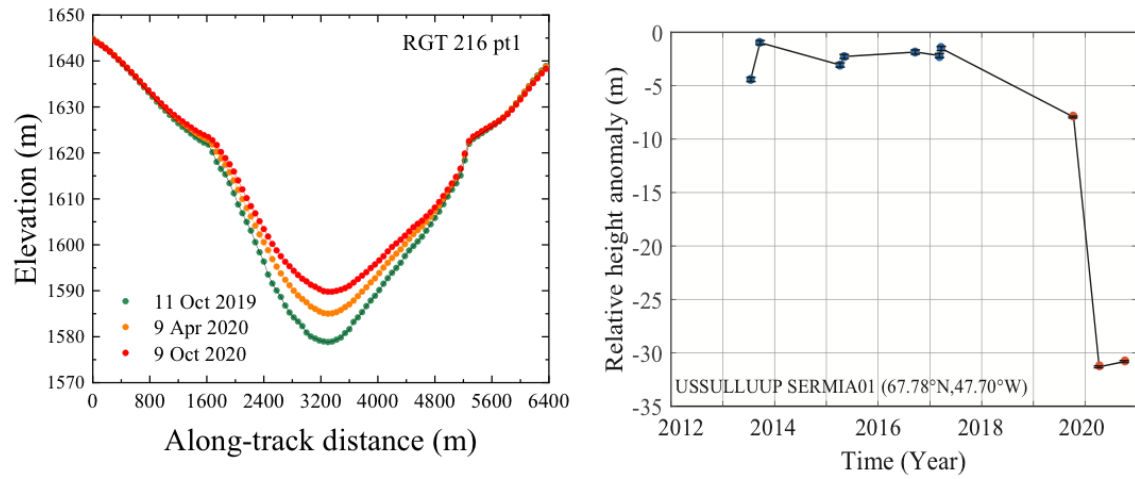


Figure S3. Elevation anomaly profile across one subglacial lake (USSULLUUP SERMIA 01) larger than 10 km². Left panel stands for the corresponding ICESat-2 RPT, and right panel stands for time series of surface height change based on ArcticDEM (blue dots) and ICESat-2 tracks (orange dots).

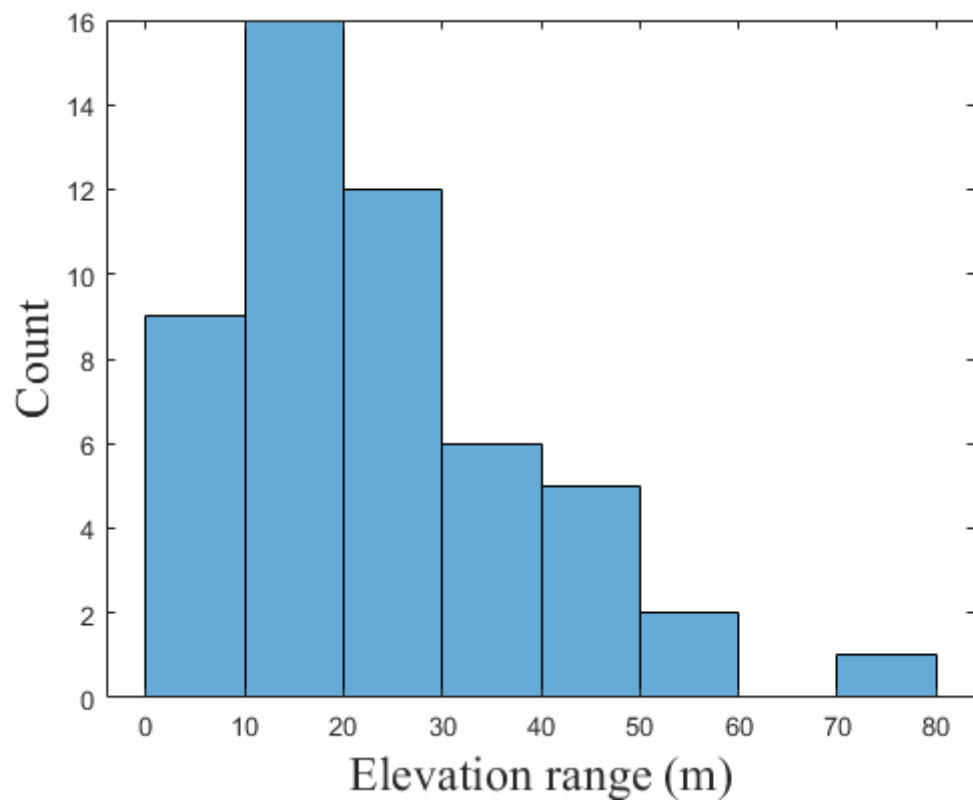


Figure S4. Histogram of elevation range of 51 lakes confirmed from the ArcticDEM, which can be used to estimate lake depth.

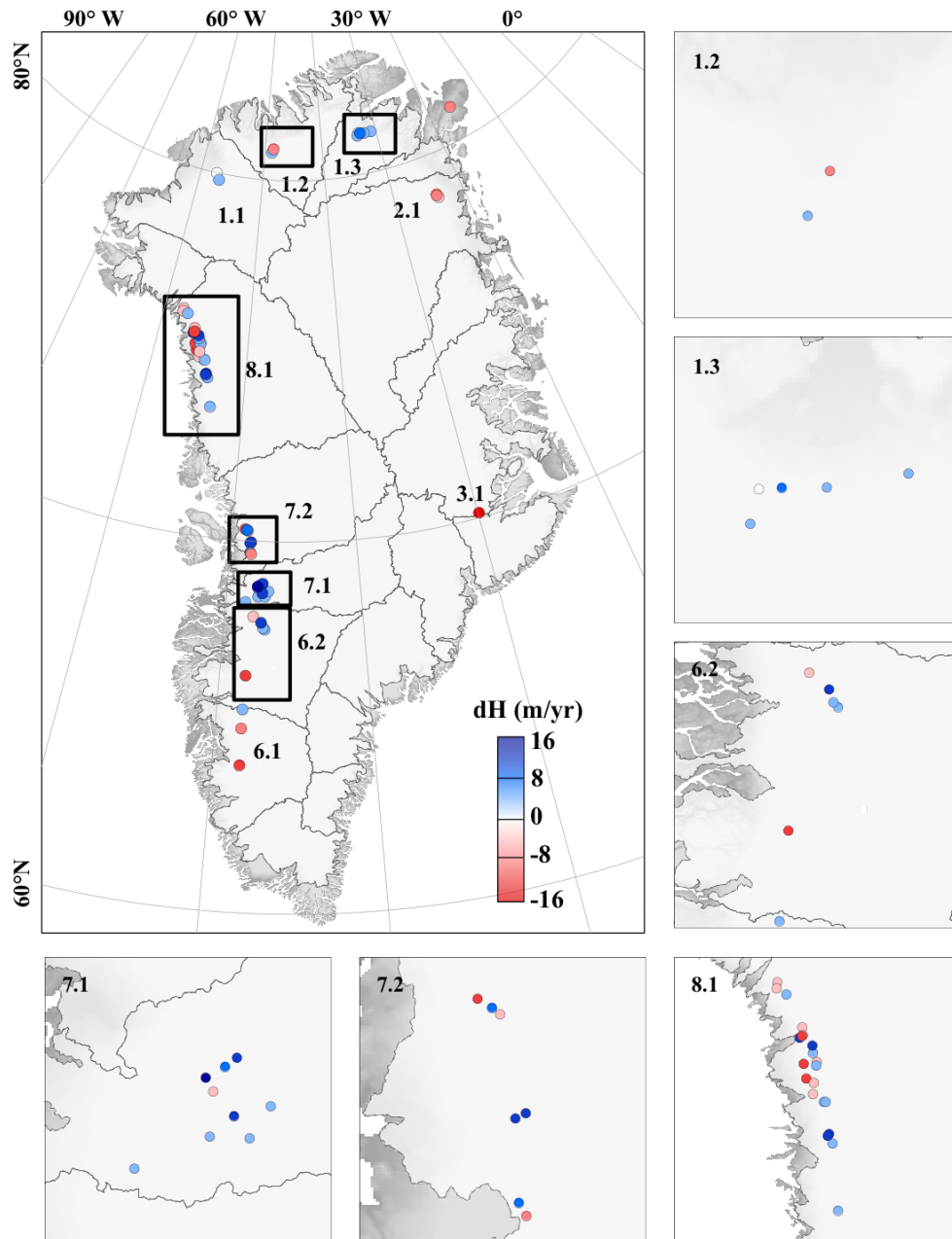


Figure S5. Elevation-change rate (dH) for the 61 subglacial lakes. These rates were derived from the slope of the best fit line to the elevation and time for each lake. The small panels exhibit six basins with large numbers of subglacial lakes.

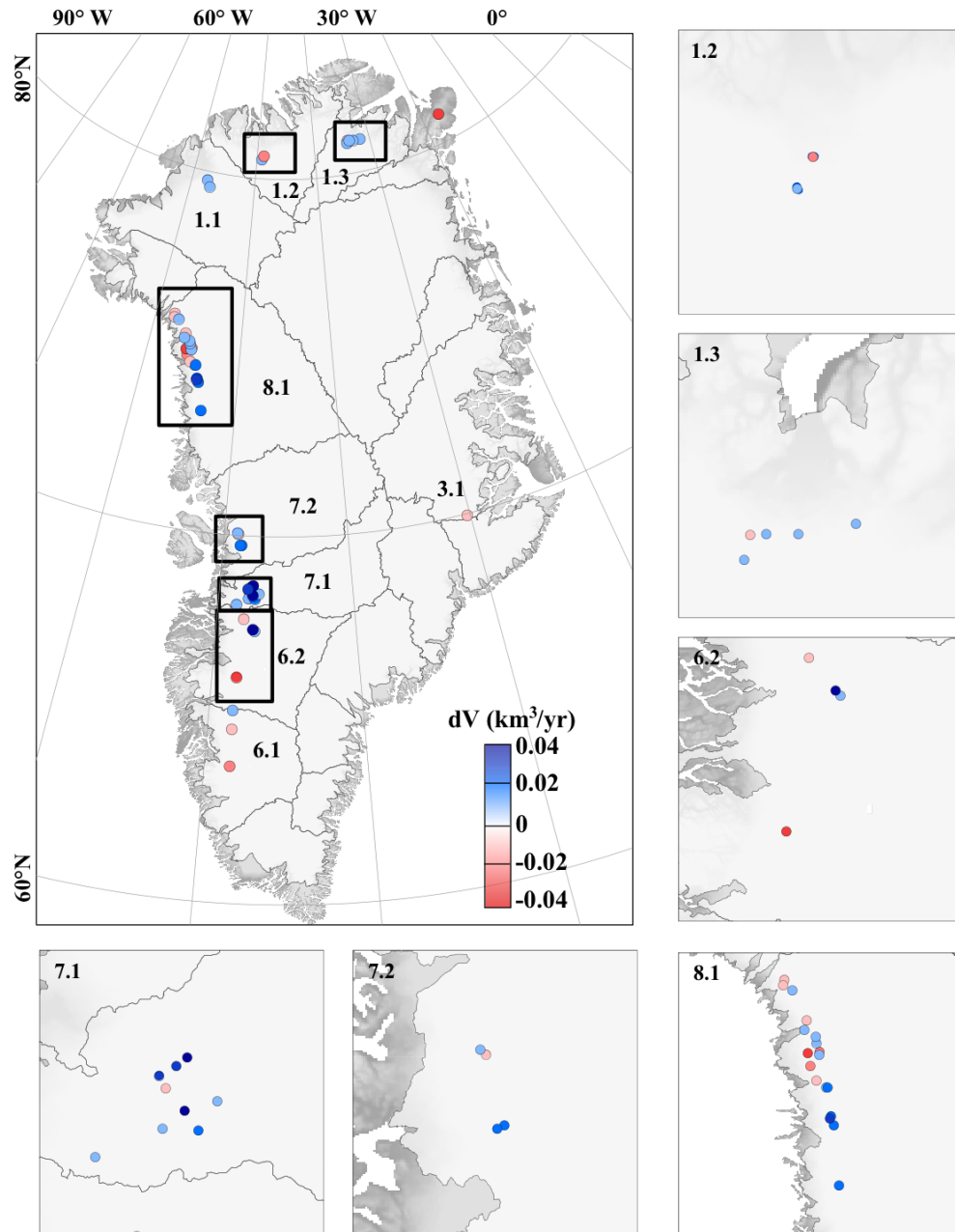


Figure S6. Volume-change rate for the 51 confirmed subglacial lakes, derived from the elevation-change rate and lake area for each lake. The small panels exhibit six basins with large numbers of subglacial lakes.

Table S1. Effects of the buffer size on lake elevation change rate for the 51 confirmed lakes. The columns give the lake name and the elevation change rate in footprints outside the bounding polygon but within the buffer zone under 3 cases. (a) A fixed buffer of 2 km, (b) the buffer of one third of the radius of the circle with an area equal to the lake area, and (c) the buffer of the radius of the circle with an area equal to the lake area.

Table S2. Parameters for all 61 lakes detected by ICESat-2 from March 2019 to December 2020. The columns give the lake name, the latitude and longitude of the lake center, the number of tracks crossing each lake, the lake area (confirmed lakes only), and the magnitude of the elevation/volume change in this 20-month period.

Table S3. Parameters for all 61 lakes detected by ICESat-2 for each activity. The columns give the lake name, the latitude and longitude of the lake center, the number of tracks crossing each lake, lake area (confirmed lakes only), the start and the end of the lake activity, and the corresponding elevation/volume change.

Table S4. Time-series elevation information for 51 confirmed lakes. The columns give mean elevation within the lake, within the lake buffer, the corresponding relative elevation anomaly, and the data acquisition date.

